

Design and Implementation of Two-Dimensional Polymer Adsorption Models: Evaluating the Stability of *Candida antarctica Lipase B* at Solid- Support Interfaces by QCM-D

Sara V. Orski,^a Santanu Kundu,^{a,†} Richard Gross,^{b,*} and Kathryn L. Beers^{a*}

^aPolymers Division, National Institute of Standards and Technology, Gaithersburg, Maryland
20899, United States¹

^bPolytechnic Institute of NYU, Brooklyn, New York 11201, United States

KEYWORDS (enzymatic polymerization, quartz crystal microbalance with dissipation, surface
adsorption, enzyme stability, lipase)

¹ This is an official contribution of the National Institute of Standards and Technology, and is not subject to copyright in the United States. Certain commercial equipment, instruments, or materials are identified in this paper in order to specify the experimental procedure adequately. Such identification is not intended to imply recommendation or endorsement by the National Institute of Standards and Technology, nor is it intended to imply that the materials or equipment identified are necessarily the best available for the purpose.

ABSTRACT

A two-dimensional model of a solid-supported enzyme catalyst bead is fabricated on a quartz crystal microbalance with dissipation monitoring (QCM-D) sensor to measure in situ stability and mechanical properties of *Candida Antarctica Lipase B* (CAL B) layers under varied conditions relating to ring-opening polymerization. The model was fabricated using a dual photochemical approach, where commercially available poly(methyl methacrylate) (PMMA) thin films were crosslinked by a photoactive benzophenone monolayer and blended crosslinking agent. This process produces two dimensional, homogenous, rigid PMMA layers which mimic commercial 3D acrylic resin in a QCM-D experiment. Adsorption of CAL B to PMMA in QCM-D under varied buffer ionic strengths produces viscoelastic enzyme layers that become rigid as ionic strength increases. The rigid CAL B/PMMA interface demonstrates up to 20 % desorption of the catalyst with increasing trace water content. Increased polycaprolactone binding at the enzyme surface was also observed, indicating higher affinity of the polymer for a hydrated enzyme surface. The enzyme layer destabilized with increasing temperature, yielding near complete reversible catalyst desorption in the model.

Introduction

The drive towards greener chemical processes has led to the development of organic and biological catalysis as environmentally favorable alternatives for the synthesis of small molecules and macromolecules. Many of these organic molecules and biological enzymes are difficult to make and purify and can result in a significant increase in production costs.¹ To sequester catalysts from reaction mixtures for easy purification and recovery, catalyst

immobilization on a solid support, or heterogeneous catalysis, has become the predominate method for straightforward catalyst separation.^{2,3}

Biodegradable polyesters have been previously synthesized by the ring-opening polymerization (ROP) of lactones using enzymatic and organic catalysts as an alternative to metal-catalyzed reactions.^{1,4} Commercially available heterogeneous catalysts (Novozyme 435, N435) have been previously utilized in batch reactors²⁻⁴ and reusable packed microfluidic columns⁵ for synthesis of polyesters with high molecular weights. N435 consists of *Candida Antarctica* Lipase B (CAL B) enzyme, immobilized on a solid support, which catalyzes the ring-opening polymerization of ϵ -caprolactone to make biodegradable polycaprolactone (PCL) and other biodegradable polyesters. CAL B immobilization occurs through physisorption at the surface of a crosslinked poly(methyl methacrylate) (PMMA) bead. Weak hydrophobic interactions between the enzyme and the surface can permit catalyst desorption, which decreases the concentration of active enzymes for polymerization and contaminates the PCL product. Better determination of conditions at the polymer/enzyme interface may enable better control of polymerization using solid-supported catalysts and improve catalyst retention for a reusable heterogeneous catalyst.

Characterization of enzymatic ROP reactions have determined that reaction conditions, such as temperature and trace water content, play a vital role in controlling polymerization kinetics and molecular weight.⁵⁻⁹ The effect of these reaction parameters, however, has varied with the configuration of the catalyst beads in batch and microfluidic reactors. Increase in polymerization temperatures in N435 batch reactors exhibited comparable polymerization rates over a 60 °C range,^{6,10} while CAL B resins in a microfluidic reactor demonstrated a noted rate increase between 55 °C to 70 °C.⁵ This disparity indicates that the stationary packing of the

heterogeneous catalyst will have an effect on the enzyme polymerization rate with increasing temperature. Direct comparison between N435 recyclability in batch and microfluidic reactors has demonstrated that microfluidic reactors are more stable under varying trace water content and will retain high conversion over several more reuse cycles with both “wet” and “dry” toluene.⁷ The stability of the immobilized enzyme catalyst under increasing temperature and water content must be understood to determine optimal conditions for the reusable solid-supported catalyst. Understanding the dynamics of the enzyme/solid support interface under varied reaction environments will help deconvolute the differences in reactor performance and enable better control of reaction rates.

Enzyme leaching occurs in both batch and packed bed microfluidic devices.^{7,8} The resulting decrease in surface catalyst concentration limits the recyclability of solid-supported catalyst. Measurement of leached enzyme is difficult in bulk polymer, however, as concentrations of enzyme relative to polymer are extremely low.⁵ Leaching of CAL B from the acrylic resin has been previously evaluated ex situ through either characterization of monomer conversion over several reuse cycles,⁵ or change in nitrogen content of the acrylic resin through elemental analysis.⁷ Catalyst leaching in these systems has been attributed to a number of causes, such as mechanical stirring and limited diffusion of water to the enzyme active sites, which is supported by the ex situ data. Stability of CAL B on the solid-support is dependent on the physiochemical interaction between CAL B and the PMMA resin interface and the mechanical stress upon the enzyme layer. The complex 3D structure of the porous bead makes systematic study of the affinity of enzyme for the PMMA surface difficult to pinpoint. A more direct and quantitative method is needed to evaluate the stability of the catalyst/polymer solid support interface

decoupled from the 3D porous resin and mechanical stresses sustained by the beads in a chosen reactor.

Biological adsorption processes at surfaces have been previously characterized by quartz crystal microbalance (QCM-D),¹¹ where protein and enzyme thin films have been formed on sensors coated with bare metal and metal oxides,^{12,13} self-assembled monolayers (SAMs)¹⁴ or spin-coated polymer thin films.^{15,16} QCM-D is a sensitive technique that can monitor small changes in resonant frequency (f) caused by adsorption of mass on the quartz sensor surface. The frequency and energy dissipation changes caused by film formation on the sensor can be used to determine mass and viscoelastic properties of the layer in real time without the need for external labels.¹⁷ Previous QCM-D studies of CAL B surface adsorption have focused on modification of surface chemistry through SAMs to control hydrophobicity.¹⁸⁻²⁰ Combinatorial studies of CAL B adsorption and activity on surface energy gradients have demonstrated surface roughness in addition to hydrophobicity will increase the binding and activity of CAL B monolayers.²¹ While these prior studies have demonstrated increased CAL B binding with hydrophobicity of the substrate, they fail to mimic the polymer microenvironment of the solid-support. The polymeric acrylic resin surface of N435, while highly crosslinked, will respond to changes in reaction environment, including swelling, changes in surface morphology, adsorption of water, and changes in viscosity and elasticity at the surface.

In this work, we developed a reproducible experimental model of the catalyst/polymer interface through fabrication of a homogenous, highly crosslinked PMMA thin film on a quartz crystal sensor. The PMMA films were covalently bound to the sensor using benzophenone as a photo crosslinker, which was 1) incorporated into the spincoated PMMA thin film and 2) covalently attached to the surface as a self-assembled monolayer (SAM). The dual

photochemical process permits efficient covalent attachment of commercially available PMMA to the surface and to other neighboring chains. The 2D mimic of the N435 enzyme solid support in a QCM-D experiment allowed for in situ changes to enzyme thin film mass and viscoelastic properties could be monitored as experimental conditions were varied. Enzyme stability was evaluated with increasing water content of toluene and polycaprolactone solutions, and with increasing reactor temperature, mimicking reaction environments where enzyme leaching and changing enzymatic activity has been previously demonstrated. This simplified 2D experimental model will permit a quantitative study of the enzyme/polymer surface microenvironment, pinpointing the sources of variation in enzyme activity (e.g. leaching versus complexed or hindered active sites). Furthermore, understanding the enzyme/polymer interface is a fundamental step in developing the next generation of biocatalysts, which are stable and recyclable for green polymer manufacturing.

Experimental

Materials. Toluene was purchased from Sigma Aldrich and distilled over CaH_2 prior to use. Poly(methyl methacrylate), number average molecular weight = $M_n = 172,000$ g/mol, polydispersity = $M_w/M_n = 1.28$, and polycaprolactone, $M_n = 10,000$ g/mol, $M_w/M_n = 1.25$ were obtained from Polymer Source. CAL B was obtained from Novozymes. QCM sensors with 50 nm SiO_2 coating (QSX303) were purchased from Q-sense. All other reagents were purchased from Sigma Aldrich and used as received.

Fabrication of Immobilized Poly(methyl methacrylate) Films. SiO_2 coated QCM crystals were sonicated in DI water for 10 min, dried under a stream of nitrogen, and subjected to ultraviolet oxygen (UVO) plasma cleaning (Jeilight UVO cleaner model 342) for 10 min to

generate a hydrophilic surface (static contact angle $< 10^\circ$). The benzophenone – terminated silane, 4-(3'-chlorodimethylsilyl)propyloxybenzophenone, was synthesized according to literature procedures.²² A 0.01 mol/L solution of the benzophenone-terminated silane in anhydrous toluene was added to Teflon-coated wells (1 cm diameter x 1 cm depth) and the QCM sensor was placed face down atop the solution to coat the SiO₂ surface only. After 16 h, the substrates were removed, rinsed with toluene, and dried under nitrogen. The benzophenone – modified sensors were then spincoated with 100 μ L of a 7.5×10^{-3} mass fraction PMMA solution in dichloroethane containing 10 mol% dibenzophenone²³ at 210 rad/s for 30 s. The sensor was transferred to a sealed Plexiglas chamber containing the UV lamp (Novacure 2100), where the chamber was purged with argon for 30 min to displace atmospheric oxygen. The PMMA film was photo-crosslinked using 345 nm light (25 mW/cm^2) for 15 min. The PMMA-crosslinked sensor was then removed from the Plexiglass chamber, rinsed with toluene to remove any unbound chains, and dried under a stream of nitrogen.

Characterization of the Crosslinked PMMA Model Surface. Film thickness of the PMMA thin films was determined by surface reflectometry on a Filmetrics reflectometer (Model F20) with a dual deuterium/halogen light source. Static water contact angles were measured on a Kruss drop shape analyzer using a 5 μ L sessile drop. Integrated software used circle fitting to determine the contact angle at the surface. Chemical composition of the PMMA crosslinked films were measured by x-ray photoelectron spectroscopy (XPS) on a Kratos Ultra DLD spectrometer using an Al K $_{\alpha}$ monochromic source (1486.6 eV) operated at 140 W. Measurements were performed at a take-off angle of 0° (normal to the surface), resulting in a depth sensitivity of (5 to 10) nm. C1s region spectra were taken on at least 6 spots per sample and 3 scans per spot to accurately sample the film. Quantification of the carbon environments

was determined by integration of fitted carbon regions by CasaXPS, using native PMMA as an original estimate for peak assignments. Surface morphology was determined using a Bruker Dimension Icon atomic force microscope (AFM). Tap 525 cantilevers with a nominal spring constant of 15 N/m were used in the PeakForce quantitative nanomechanical measurements (QNM) to determine film elasticity. All thickness, contact angle and PeakForce QNM measurements were performed at least three times and the error reported with all measurements represents one standard deviation between trials.

General Description of Adsorption Monitoring through Quartz Crystal Microbalance with Dissipation (QCM-D). QCM-D was performed using a Q-Sense E4 module controlled by Q-Soft integrated software. Two QCM modules were connected in parallel for enzyme/PMMA and PMMA control samples for all experiments unless otherwise indicated. Baseline measurements were taken after 30 minutes of equilibration of each module at $22\text{ }^{\circ}\text{C} \pm 0.5\text{ }^{\circ}\text{C}$ in the desired solvent at a flow rate of $100\text{ }\mu\text{L}/\text{min}$ using a peristaltic pump (Ismatec N4). After the reaction was complete, solvent was reintroduced into the modules to rinse any loosely adsorbed analytes and the final frequency and dissipation changes were determined. All QCM-D experiments were performed at least three times and all error bars on experimental and calculated data represent one standard deviation between all trials.

Monitoring of CAL B Adsorption through Quartz Crystal Microbalance with Dissipation (QCM-D). Two PMMA-modified quartz crystal sensors were equilibrated in 0.10 mol/L phosphate buffer (pH 7.0). Enzyme solution of 0.2 mg/mL CAL B in phosphate buffer was added to one of the modules and enzyme adsorption was monitored. After the baseline stabilized indicating no further enzyme adsorption, buffer was flowed through the cell to remove any

loosely bound enzymes and to establish the final enzyme concentration at the PMMA surface. Buffer salts were removed from the CAL B layer by rinsing nanopure DI water through the module. Minimal loss of the enzyme was observed (< 3 %) with the water rinse, as changes in frequency and dissipation were due to viscosity changes between buffer and water, and were consistent with control samples. The PMMA surface exposed only to buffer was used as the control samples for all further studies.

Monitoring of CAL B Stability with Increasing Water Content of Organic Solvent by QCM-D. Baseline measurements for enzyme/PMMA and PMMA samples were taken in toluene (water mass fraction of 250 ppm). The water study occurred through successive addition of toluene with higher water fractions to both the enzyme and control samples from 250 ppm, 350 ppm, and 450 ppm concentrations, where all water concentrations, as measured by KF coulometric titration, were within ± 6 ppm. Each toluene solution flowed through the modules until frequency and dissipation values remain unchanged. Water content of the toluene solutions were measured by Karl Fischer coulometric titration. Changes in frequency and dissipation with time were recorded for each sensor.

Monitoring in situ Polycaprolactone Adsorption on CAL B Thin Films by QCM-D. Baseline measurements for enzyme/PMMA and PMMA samples were taken in toluene (water mass fraction of 250 ppm). Polycaprolactone solutions in toluene (5.5×10^{-3} mol/L) containing water mass fractions of (250, 350, and 450) ppm were prepared. The water content of all PCL solutions were within 10 ppm of the toluene solutions from the above study. The 250 ppm PCL solution was added to the modules, followed by the 350 ppm and 450 ppm PCL solutions. The experiment was complete within 3000 s. Saturated toluene (450 ppm) was then added to the modules to remove any unbound PCL.

Monitoring of CAL B Thermal Stability through High Temperature Quartz Crystal Microbalance with Dissipation (HT-QCM-D). A single enzyme/PMMA sensor was sealed in a high temperature QCM-D module within a Teflon block and allowed to equilibrate in toluene (300 ppm water content). The peristaltic pump was stopped and static toluene remained in the module. This baseline response was recorded for 20 min. The temperature of the HT-QCM-D module was gradually increased to 30 °C by an integrated Q-soft temperature program at a rate of 3.33 °C/min and held constant for 20 min. The program continually raised the cell temperature by 10 °C at 20 minute intervals using the aforementioned ramp rate, until the cell reached 90 °C. A longer ramp time (\approx 20 min) was required to reach the final 90 °C temperature within the module. The cell was then cooled back to 22 °C and allowed to run overnight. The experiment was repeated with PMMA modified crystals and unmodified SiO₂ crystals as control samples.

Monitoring of Influences of Buffer Ionic Strength on CAL B Adsorption by QCM-D. Phosphate buffer solutions (pH 7.0) were made with salt concentrations of (0.010, 0.020, 0.040, 0.060, 0.080, and 0.100) mol/L. Corresponding buffer solutions containing 0.2 mg/mL CAL B enzyme were made by serial dilutions using a 0.2 mg/mL enzyme in 0.100 mol/L buffer stock solution and a 0.2 mg/mL water solution to ensure enzyme concentration was equivalent between all ionic strength solutions. For each buffer studied, a crosslinked PMMA sensor was sealed within a QCM-D module and equilibrated in buffer. The 0.2 mg/mL CAL B solution in the appropriate buffer was then added until no additional adsorption was observed.

Modeling of Enzyme Mass Surface Coverage and Viscoelastic Properties by Quartz Crystal Microbalance with Dissipation (QCM-D). Characterization of the mass and mechanical properties of the enzyme layer is dependent on the oscillation behavior of the thin film formed

relative to the quartz sensor. It is important to note that QCM-D will determine the mass of the solvated layer at the crystal. When the adsorbed layer is rigid and oscillates with the crystal, mass can be calculated proportionally to the frequency change, known as the Sauerbrey relationship.²⁴ When the enzyme layer is non-rigid (viscoelastic), there will be a change in dissipation energy of the oscillating crystal. The simultaneous changes in frequency and dissipation monitored by QCM-D can be used to characterize the mechanical properties of the film through application of Voigt-Kelvin viscoelastic models.²⁵ An extensive discussion of QCM-D theory and adsorption modeling parameters are available in the literature.^{17,26,27}

All changes in frequency and dissipation with time were recorded for all QCM-D samples. The changes in frequency discussed throughout in this work are normalized frequency changes, $\Delta f_n/n$, where the frequency of a given overtone, n , is divided by the overtone number to compare frequency changes between overtones. Overtone frequency and dissipation responses were recorded for the fundamental frequency ($f_1 = 5$ MHz) and the 3rd, 5th, 7th, 9th, 11th, and 13th overtones ($f_n = n f_1$). Viscoelastic modeling was restricted to the 3rd through 5th overtones in this study to assess changes at the PMMA/CAL B interface across the greatest crystal area, but to avoid crystal mounting stresses that can affect responses in f_1 . Determination of areal mass of the resultant enzyme films is dependent on the frequency and dissipation response of the enzyme layer under varied reaction conditions. In a rigid system, the change in dissipation (ΔD_n) is much less than the frequency change. A ratio of $\Delta D_n/(-\Delta f_n/n) \ll 4 \times 10^{-7}$ is indicative of a rigid layer.¹⁷ When the adsorbed layer behaves as a rigid solid, the areal mass is determined by the Sauerbrey equation (Equation 1), where n is the overtone and C is a constant dependent on crystal properties, which is $17.7 \text{ ng cm}^{-2}\text{Hz}^{-1}$.

$$\Delta m = -\left(\frac{C}{n}\right) \Delta f \quad (1)$$

For non-rigid films, the dissipation factor, D , describes the sum of dissipated energy of the oscillation.

$$D = \frac{E_{dissipation}}{2\pi E_{stored}} \quad (2)$$

Changes to frequency and dissipation can be used to determine properties of the film such as thickness, density, shear viscosity, and shear elasticity by using a Kelvin-Voigt mechanical model (equation 3), that describes a viscoelastic solid as an elastic spring and viscous dashpot connected in parallel. A Taylor expansion of the Kelvin-Voigt model has been previously determined by Voinova and coworkers²⁵ to fit frequency and dissipation changes to viscoelastic properties, and is included below:

$$G^* = G' + iG'' = \mu + i2\pi f\eta, \quad i = \sqrt{-1} \quad (3)$$

$$\Delta f \approx \frac{1}{2\pi\rho_Q h_Q} \left\{ \frac{\eta_b}{\delta_b} + h\rho\omega_n - 2h \left(\frac{\eta_b}{\delta_b} \right)^2 \frac{\eta\omega^2}{\mu^2 + \omega^2\eta^2} \right\} \quad (4)$$

$$\Delta D \approx \frac{1}{\pi f\rho_Q h_Q} \left\{ \frac{\eta_b}{\delta_b} + 2h \left(\frac{\eta_b}{\delta_b} \right)^2 \frac{\eta\omega}{\mu^2 + \omega^2\eta^2} \right\} \quad (5)$$

where G^* is the complex shear modulus, G' is the storage modulus, G'' is the loss modulus, μ is the shear elasticity, f is the measured frequency, and η is the shear viscosity in equation 3. For the frequency (equation 4) and dissipation (equation 5), h is the film thickness, ρ is film density and h_Q and ρ_Q are the thickness and density of the quartz sensor, respectively, η_b and δ_b denote the bulk fluid viscosity and viscous penetration depth of shear wave in the bulk fluid. The angular frequency, ω , is equal to $2\pi f_n$. These equations are simultaneously fit in Q-tools software (Q-sense) to determine μ , η , the Voigt mass ($h\rho$), and the accuracy of the fit (χ^2). The Kelvin-Voigt model assumes a Newtonian bulk fluid where solution viscosity is independent of

frequency. An enzyme density of 1200 kg/m^3 was assumed for all viscoelastic modeling in this work, which has been used to estimate previous hydrated enzyme layers.²⁸

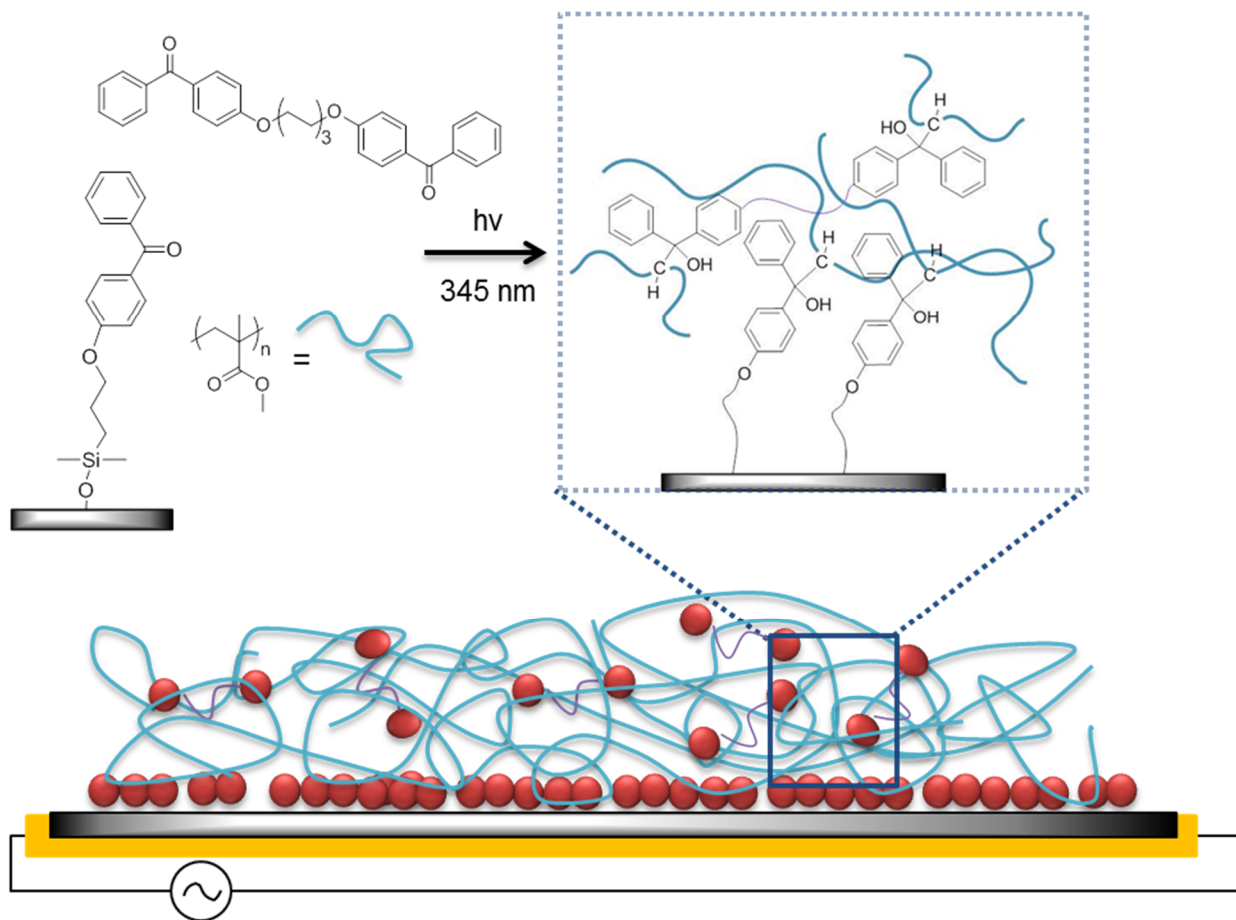
Results and Discussion

Development and Characterization of the Two-Dimensional PMMA QCM-D Model System.

Evaluation of enzyme stability was measured using QCM-D to detect sensitive mass changes of the enzyme adsorbed on the PMMA support in situ. In a typical QCM experiment, a voltage is applied to an AT-cut quartz crystal, which causes it to oscillate at a fundamental frequency ($f_1 = 5 \text{ MHz}$). The CAL B film formed on the modified crystal surface will decrease the resonant frequency; this change can be used to calculate mass adsorbed on the sensor. Adsorbed enzyme should be evenly distributed and the surface should have a high degree of lateral homogeneity to determine accurate mass changes from frequency measurements.

The crosslinked PMMA model surface was fabricated on a quartz crystal sensor through a dual photochemical approach, using a photoactivated benzophenone crosslinker as both a SAM and as an additive within the polymer thin film. This strategy crosslinks the PMMA to the surface and to neighboring chains.²⁹ Copolymers with benzophenone-modified pendant groups have been previously immobilized at the surface through mild UV irradiation without oxidative degradation of the polymer.^{22,30–35} Other commercially available polymers can be synthesized, characterized, and crosslinked to the QCM sensor surface using identical SAM formation procedures and incorporation of dibenzophenone crosslinking agent, only optimizing for spin-coating conditions of the polymer layer. A representation of the crosslinked PMMA sensor is shown in Scheme 1.

Scheme 1. Depiction of two-dimensional crosslinked PMMA thin film on quartz crystal sensor (side view).



PMMA chains are represented by blue lines and benzophenone moieties are represented by the red dots. The schematic is not to scale.

The original PMMA spincoated films were $52 \text{ nm} \pm 2 \text{ nm}$ thick which decreased to $50 \text{ nm} \pm 3 \text{ nm}$ after crosslinking, indicating no significant change in film thickness upon UV irradiation. The static contact angle of the PMMA films before and after UV irradiation was $80^\circ \pm 2^\circ$ and $78^\circ \pm 2^\circ$, respectively, indicating no significant change in hydrophobicity of the PMMA layer. No change in film thickness or contact angle of the substrates was observed after Soxhlet extraction in THF (16h), indicating a highly crosslinked, stable PMMA layer. The large concentration of benzophenone crosslinker in PMMA film, 10 mol% relative to monomer, was

used to increase the crosslinking density, therefore ensuring minimal swelling of the model thin film. The crosslinked PMMA layer, as a result, oscillated with the quartz sensor as a rigid film in QCM-D. This high concentration of crosslinker did not significantly alter the hydrophobicity of the surface as the resulting contact angle post-crosslinking was equivalent to bulk (non-cross-linked) PMMA measurements.

Confirmation of the crosslinked PMMA surfaces were evaluated by XPS. The C1s region of benzophenone-PMMA films before and after UV irradiation were measured and carbon chemical shifts were identified by peak fitting using Casa XPS software. A summary of peak fitting results is shown in Table 1. UV irradiation of the PMMA film results in a 4.7 % decrease in C-H bonds in the film (285.01 eV, red curve in Figure 1a and 1b) and a 4.9 % increase in C-C bonds adjacent to oxygen (285.78 eV, blue curve). The C1s peak at 285.78 eV represents both C-C-OH from crosslinking with C-C=O from PMMA. This measurement is consistent with the theoretical change in carbon environment with photoactivation of the benzophenone sites within the film.

Table 1. Assignments of C1s XPS spectra for non-crosslinked and crosslinked PMMA films containing 10 mol% dibenzophenone crosslinker.

C1s Assignment	Position (eV)	% Area Before	% Area After
		Crosslinking	Crosslinking
CH	285.01	50.36	45.42
C=O	289.11	15.02	15.14
C-O	286.75	24.03	24.15
C-C-OH/ C-C=O	285.78	10.58	15.30

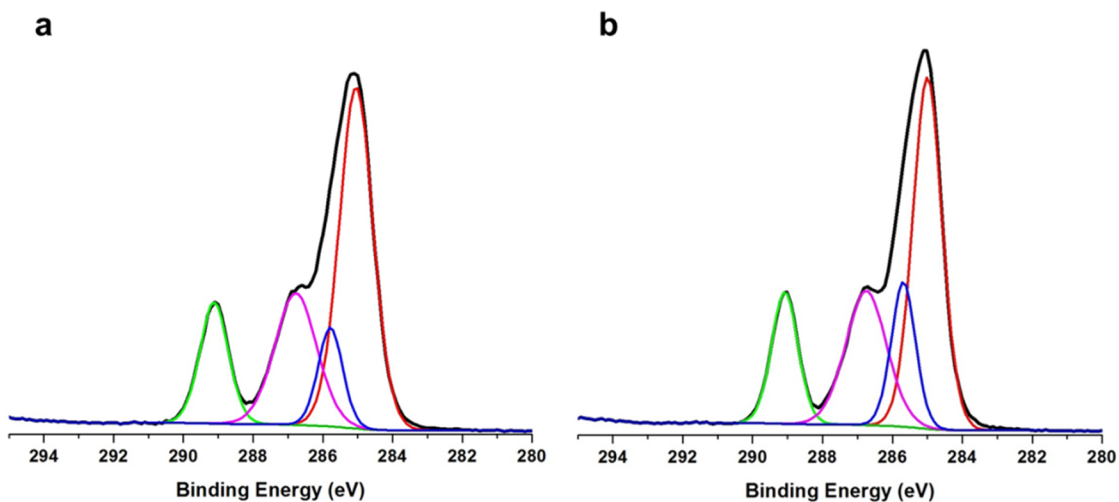


Figure 1. C1s XPS spectra of 50 nm PMMA thin films with 10 mol% benzophenone crosslinking agent before (a) and after (b) UV irradiation. The black line is the original spectra and the binding energy maxima at (289.11, 286.75, 285.78, and 285.01) eV represent the fit of the C=O, C-O, C-C-OH/ C-C=O, and C-H binding energy contributions, respectively.

The PMMA-modified quartz sensor surface was also evaluated by AFM Peak Force QNM sensing (Bruker) to determine surface roughness and Young's modulus of the film. Surface homogeneity is critical to deconvolute effects of the chemical interaction of the enzyme/polymer interface from physical interactions such as porosity, and to obtain accurate QCM-D data. An AFM height image (3 μm x 3 μm scale) of the crosslinked PMMA surface (Figure S1 of the supporting information) indicates a very smooth film, with an RMS roughness of 0.46 nm, and minimal defects within the film. The modulus of the film was determined by a relative method, where the cantilever spring constant and tip radius was measured on a thin film polystyrene standard.³⁶ The PMMA sensor surface is highly rigid once crosslinked, with a Young's modulus of 8.2 GPa \pm 0.4 GPa, as compared to 2.5 to 5.0 GPa for bulk non-crosslinked PMMA.³⁷⁻³⁹

Adsorption of *Candida Antartica Lipase B* (CAL B) on PMMA sensor model.

Adsorption of CAL B on the PMMA surface occurs rapidly as 90 % of the enzyme adsorption is complete within 300 s of addition to the flow module. Continuous flow of the enzyme solution continued until frequency response stabilized ($\Delta f_n = 0$), indicating no further enzyme adsorption. Buffer rinsing resulted in a 13.8 % \pm 5 % mass loss ($85 \text{ ng/cm}^2 \pm 31 \text{ ng/cm}^2$) due to the removal of weakly attached enzyme. The CAL B layer adsorbs as a rigid solid, indicated by the identical changes in frequency on all overtones ($n = 3, 5, 7, 9, 11$) with a small dissipation value of 1.0×10^{-6} . Frequency and dissipation changes for the enzyme adsorption are shown for the 3rd, 5th, and 7th frequency overtone in Figure S2 of the supporting information. The mass of the CAL B layer was calculated using the 3rd overtone ($f_3 = 15 \text{ MHz}$) by the Sauerbrey equation (Equation 1), yielding a final mass surface coverage of $530 \text{ ng/cm}^2 \pm 63 \text{ ng/cm}^2$. The Sauerbrey mass increase throughout the adsorption process is shown in Figure 2 with solution transitions highlighted by the red arrows.

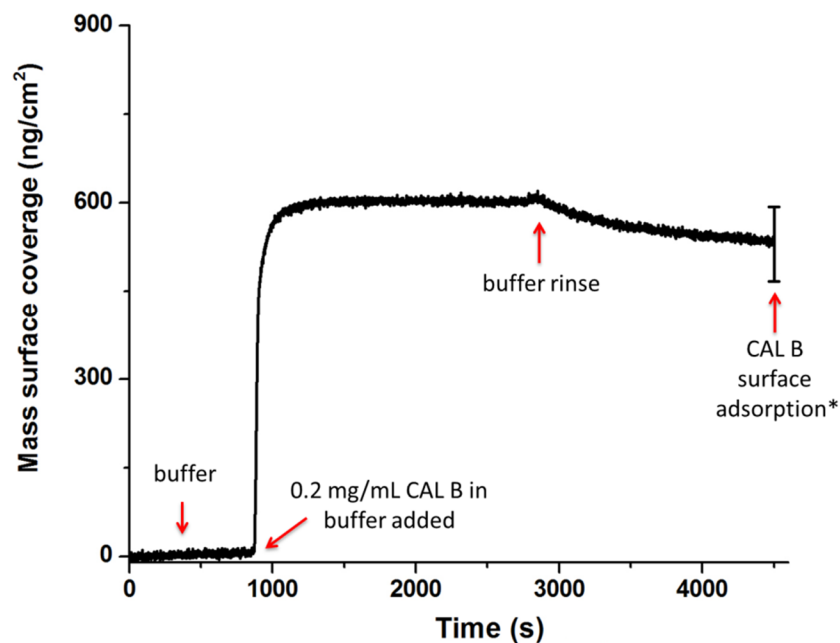


Figure 2. Adsorption of CAL B mass on a PMMA crosslinked QCM-D sensor in 100mM phosphate buffer (pH 7.0). Final mass surface coverage (*) of CAL B is calculated after buffer rinse.

Effects of Water Concentration on Interfacial Stability of CAL B.

CAL B catalyst stability was evaluated in toluene with increasing water concentrations from 250 ppm to 450 ppm. This range was used to evaluate CAL B at the PMMA model surface over a similar water content range used for kinetic evaluation of ϵ -CL polymerization under “dry” (anhydrous monomer removed) and “wet” reaction conditions of 347.4 ppm (0.0193 mol/L) and 383.4 ppm (0.0213 mol/L), respectively.⁸ The significant amount of water retained in the beads likely explains the small difference in “dry” versus “wet” reaction conditions. Anhydrous conditions (37.8 ppm, 0.0021 mol/L), where all water was removed from the enzyme beads, were not duplicated in this study due to low total conversion for the dehydrated enzyme catalyst.⁸

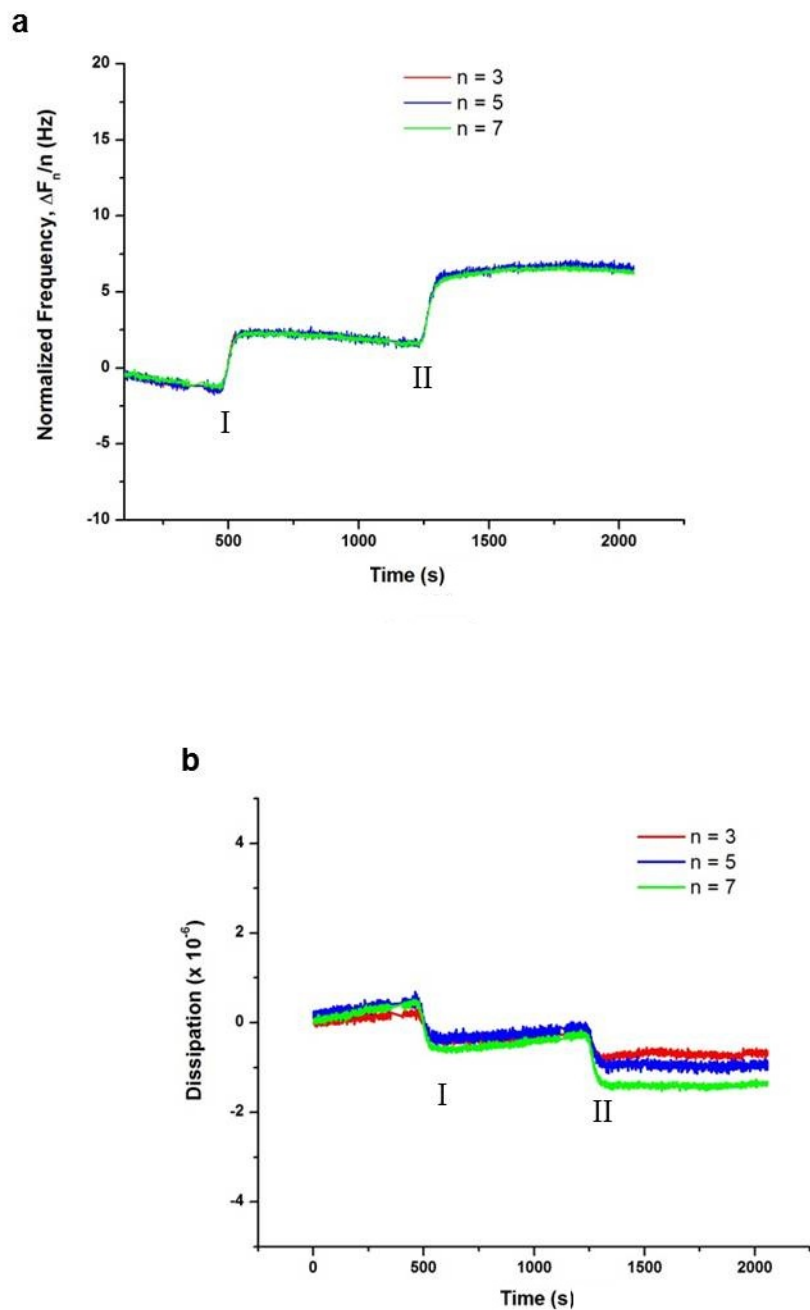


Figure 3. Representative in situ frequency (a) and dissipation (b) changes for overtones 3, 5, and 7 to CAL B modified PMMA surface in toluene with increasing water content from (250 to 350) ppm (I) and (350 to 450) ppm (II).

Frequency increases identically for all overtones with the increase of water content in toluene at 350 ppm and 450 ppm (Figure 3a) for the CAL B modified PMMA sensor. Dissipation also decreased identically for the frequency overtones with 350 ppm water in toluene (Figure 3b). The spreading of overtones 3, 5, and 7 for dissipation at 450 ppm water indicates a decrease in rigidity of the surface. Viscoelastic modeling, however, of the 350 ppm to 450 ppm transition yielded no significant change in the Voigt mass versus the Sauerbrey mass. These values and the identical change in frequency for all overtones during the study indicated that enzyme layer remained mostly rigid and was therefore modeled by the Sauerbrey equation (equation 1). The PMMA control samples demonstrated no significant change in dissipation ($0 - 0.5 \times 10^{-6}$) for the entire experiment. Frequency response of the PMMA control surface was identical for all measured overtones, where the only change observed was a 1 Hz ($\sim 20 \text{ ng/cm}^2$) decrease with addition of 450 ppm solution, indicating a small mass increase of the sample due to water adsorption on the PMMA surface.

Sauerbrey calculations yield a decrease in mass surface coverage of the enzyme of $40 \text{ ng/cm}^2 \pm 7 \text{ ng/cm}^2$ at 350 ppm water concentration and a further decrease at 450 ppm water in toluene leading to a total mass loss of $101 \text{ ng/cm}^2 \pm 26 \text{ ng/cm}^2$. Figure 4 depicts the mass loss with increasing water content of the CAL B layer at 350 ppm (I) and 450 ppm (II) with only a slight increase of 20 ng/cm^2 for the control sample, due to water adsorption on the PMMA layer. These results indicate an 8 % mass loss of CAL B on the PMMA solid support under “dry” ring-opening polymerization conditions ($< 347.4 \text{ ppm water}^8$) using N435 catalyst beads. Further increase of the water content to “wet” polymerization conditions ($> 382.7 \text{ ppm water}^8$) results in a loss of up to 20.2 % of total CAL B mass from the support resin. The CAL B leaching from the surface is attributed to water absorption by the enzyme, yielding a softer CAL B layer and

disrupting the hydrophobic interaction between the enzyme and the PMMA surface. The leaching of CAL B is only a fraction of available enzyme on the surface, but will contaminate the PCL product and decrease remaining catalyst concentration within the N435 resin.

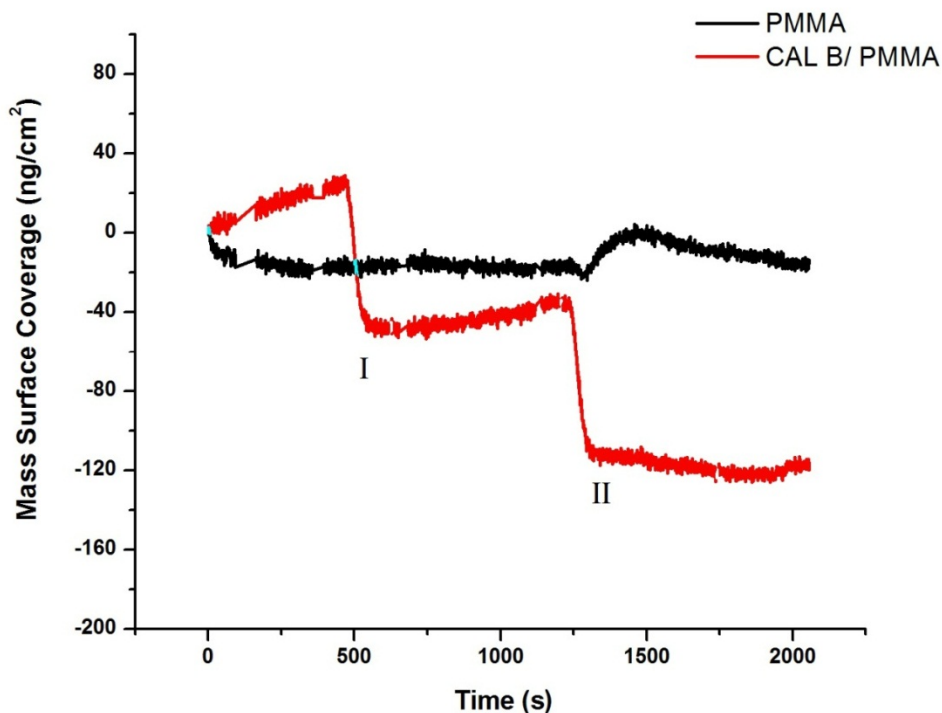


Figure 4. Mass loss of adsorbed CAL B enzyme (red) due to increasing water concentration at 350 ppm (I) and 450 ppm (II) transitions over control PMMA (black). Sauerbrey mass surface coverage was calculated using f_3 overtone.

Effect of Water Concentration on Formation of the Polycaprolactone-Enzyme Complex.

Adsorption of polycaprolactone to CAL B with increasing water content was also evaluated under flow conditions for ϵ -CL polymerization. A solution of PCL ($M_n = 10,000$ g/mol) with increasing water content was added to the CAL B modified PMMA model to determine how the added presence of water would affect the enzyme-polymer complex

for ROP. The addition of the PCL will cause a viscoelastic response in QCM-D from the increase in solution viscosity and adsorption of PCL at the surface. Changes in mass adsorption due to enzyme must be evaluated as the difference between enzyme modified and unmodified PMMA to deconvolute the mass change of the enzyme-polymer complex from non-specific binding of PCL to the surface. The frequency changes for the 3rd, 5th, and 7th overtones for CAL B and PMMA sensors are shown in Figure 5. There is a steady decrease in frequency response in both surfaces due to continuous adsorption of PCL onto the sensors. The difference in frequency and dissipation for the 3rd, 5th, and 7th overtones was calculated and fitting was attempted using Kelvin-Voigt viscoelastic models. Due to the very small changes in frequency and dissipation for the difference data, a good fit of viscosity or storage modulus could not be obtained. The mass change due to the enzyme-polymer complex was therefore estimated by the Sauerbrey relationship and is summarized in Table 2. Distinct transitions occur in enzyme/PCL binding where the water content is increased by 100 ppm, as seen in Figure 5 (blue curve). The mass due to binding of polymer to CAL B increases between 250 ppm and 350 ppm by an average of 29.2 ng/cm² and the average PCL binding to CAL B remains constant for the increase to 450 ppm among repeat trials. The Sauerbrey mass for the 450 ppm transition is slightly underestimated relative to the mass obtained from a viscoelastic model fit.

The increase in PCL binding to CAL B with additional water content appears inconsistent with the enzyme loss observed with water concentration in toluene. The small decrease in frequency of the CAL B layer indicates that enzymes forming active complexes with PCL will not desorb from PMMA to the same extent we observe in the prior study. Quantitative proof, however, cannot be obtained due to experimental limitations of QCM-D. For the reaction system, the mass loss of the enzyme and the addition of PCL to the remaining enzymes are convoluted in a single

modeled layer and compared to PMMA controls. There is an increase in mass of the PCL/CAL B layer on the PMMA surface during the 250 ppm to 350 ppm transition, however there was no statistically significant change in the transition from 350 ppm to 450 ppm.

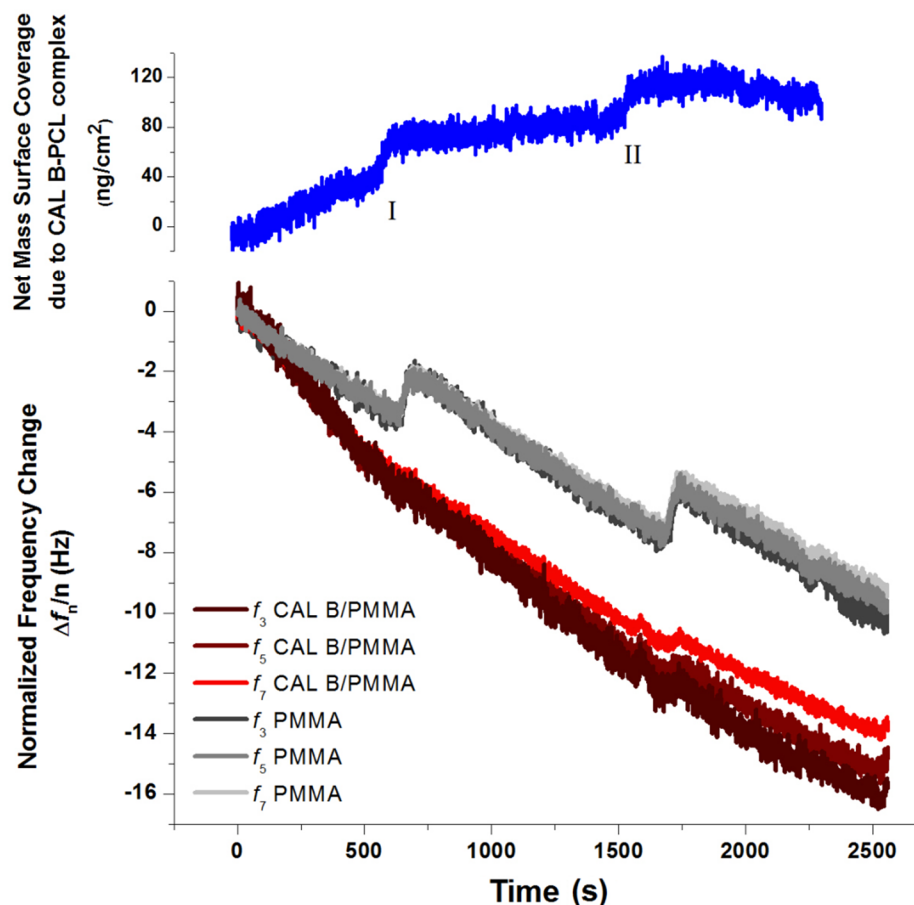


Figure 5. Changes in frequency ($n = 3, 5, 7$) for CAL B/PMMA and PMMA modified sensors upon addition of polycaprolactone solutions (5.5×10^{-3} mol/L) containing 250 ppm ($t=0$), 350 ppm (I) and 450 ppm water (II). The Sauerbrey mass change due to PCL adsorption to enzyme is calculated by difference in f_3 for the enzyme and control samples (blue).

Table 2. Average Mass Surface Coverage of CAL B/PCL complex with increasing water content.

5.5×10^{-3} mol/L PCL solution in toluene containing X ppm water	Average Change in Mass Surface Coverage due to the CAL B-PCL Complex (ng/cm²)
250 ppm	58.3 ± 16
350 ppm	87.5 ± 3.0
450 ppm	87.9 ± 12

PCL reaction kinetics have been studied and modeled as a function of water concentration.^{8,9} Indeed, water concentration has been demonstrated to be critically important to the concentration of free polyester chains in solution and to the equilibrium between the enzyme catalytic function to polymerize or degrade chains.^{8,9} For experiments and models of N435-catalyzed ROP of ϵ -CL in solution,⁸ the increase in water concentration will result in more free enzyme active sites, as water catalyzes the hydrolysis of the PCL-enzyme ester bond, releasing a free PCL chain. At 250 ppm, where the toluene and PCL are dry and the enzyme is more dehydrated than on unmodified N435 beads, propagation is slower and the residence time of a PCL chain bound to a CAL B active site is increased. By increasing the water concentration, the turnover rate of CAL B increases and more active sites for PCL binding are available. This creates increased diffusion of PCL chains to active CAL B enzymes and therefore a greater mass at the sensor surface. Prior PCL/CAL B kinetic models have determined the effects of net water concentration in the reaction system, but could not account for the affinity of water between CAL B and PCL.⁸ The observed continuous adsorption onto the PCL/PMMA layer indicates that water affinity may sequester PCL chains near the enzyme surface. Further QCM-D studies

replicating PCL binding to the CAL B/PMMA model under turbulent flow profiles may determine whether mechanical stress on the catalyst surface will overcome water affinity between CAL B and PCL chains.

Evaluation of CAL B Stability with Reaction Temperature.

The PMMA/CAL B interfacial stability was also evaluated as a function of temperature. A bare SiO₂ crystal in addition to PMMA and CAL B-modified PMMA sensors were equilibrated in a high temp QCM-D with 300 ppm trace water content in toluene. A temperature program increased the module temperature in 10 °C intervals from 22 °C to 90 °C, holding at each temperature for 20 min to establish equilibrium, then returning to 22 °C. The frequency response of the 3rd overtone with time during the temperature ramp is shown in Figure 6. It is necessary to conduct control samples on bare crystals in addition to the PMMA controls due to the frequency and dissipation dependence of the quartz crystal on the temperature of the experiment.^{40,41} In addition, the density and viscosity of toluene are also dependent on temperature and are documented in the literature.^{42,43} To account for frequency changes due to the crystal and toluene at elevated temperatures, it is necessary to correct frequency and dissipation responses of the PMMA and CAL B/PMMA temperature experiments by subtraction of the bare crystal. These corrected values as a function of temperature are shown in Figures S3a and S3b of the supporting information.

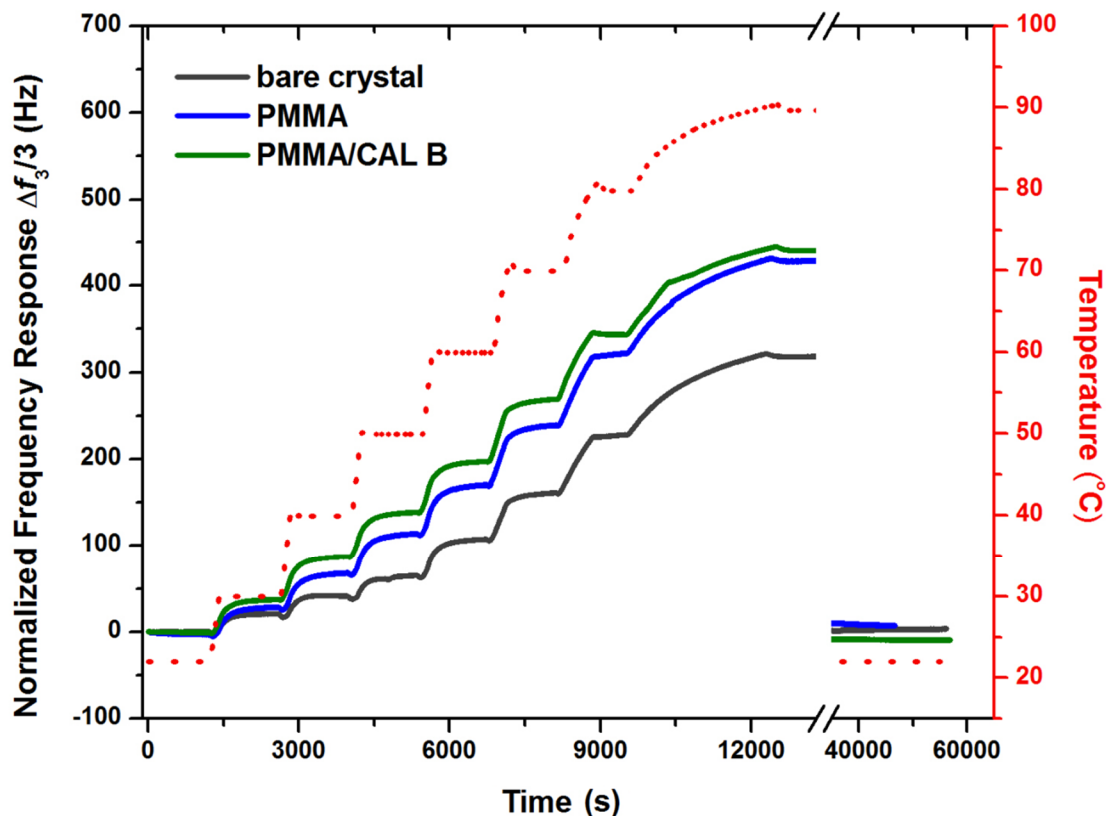


Figure 6. Changes in the 3rd frequency overtone (15 MHz) for CAL B/PMMA, PMMA, and bare quartz crystal sensors in toluene (300 ppm water) with increasing temperature (red dashes).

Voigt viscoelastic fits were attempted with the corrected CAL B data, using both an extended viscoelastic model^{17,27} option to model the frequency dependence of G' and η and standard Kelvin-Voigt models.^{27,41} The inability to converge on a reasonable viscoelastic fit is due to the smaller magnitude of dissipation changes relative to frequency for the corrected CAL B layer. Generally, if the ratio of $\Delta D_n / (-\Delta f_n/n) \ll 4 \times 10^{-7}$,¹⁷ the layer on the sensor can be approximated as rigid. The ratio was calculated for the third overtone of the CAL B data at each temperature and is summarized in Table S1 of the supporting information. The ratio of $\Delta D_n / (-\Delta f_n/n)$ for CAL B is right at the approximation threshold, where the film can be

approximated as rigid below 50 °C, and viscoelastic above. The CAL B layer thereby remains mostly elastic, with minimal diffusion and relaxation occurring between the surface-bound enzymes. Voigt modeling for these experiments may also yield a poor viscoelastic fit due to the experimental constraints of the reaction; the correction between bare crystal, PMMA, and CAL B/PMMA in our experiments were conducted on crystals from the same lot, but not on a single crystal. This was due to concerns about hysteresis of the crosslinked PMMA control film swelling at high temperatures, then being reused to deposit CAL B.

Mass changes of CAL B, independent from the PMMA support layer, were determined by the net change in frequency and dissipation for each overtone from the unmodified PMMA layer. The determination of mass of the CAL B layer was calculated from the corrected 3rd overtone by the Sauerbrey model (Figure 7). The error bars of the calculated mass are representative of one standard deviation between repeated trials. Mass surface coverage of the CAL B layer decreases with increasing temperature; by 60°C, there is a 40% decrease in CAL B mass and 90% of the enzyme layer is desorbed by 90 °C. The frequency and dissipation changes of the CAL B/PMMA and PMMA layers (Figure S3a and S3b) indicate that the Sauerbrey model may be an underestimate at temperatures greater than 50 °C, with the most uncertainty at 80 °C - 90 °C, where the divergence in frequency and dissipation of frequency overtones is highest. Increasing temperature disrupts the CAL B layer, permitting enzyme diffusion from the PMMA surface, which is reversible upon cooling. Mass decrease may be attributed, in part, to dehydration of CAL B with increasing temperature. Enzyme dehydration, however, will only account for a small fraction of the mass loss, however, as only water at the enzyme surface can be removed by organic solvents.⁴⁴

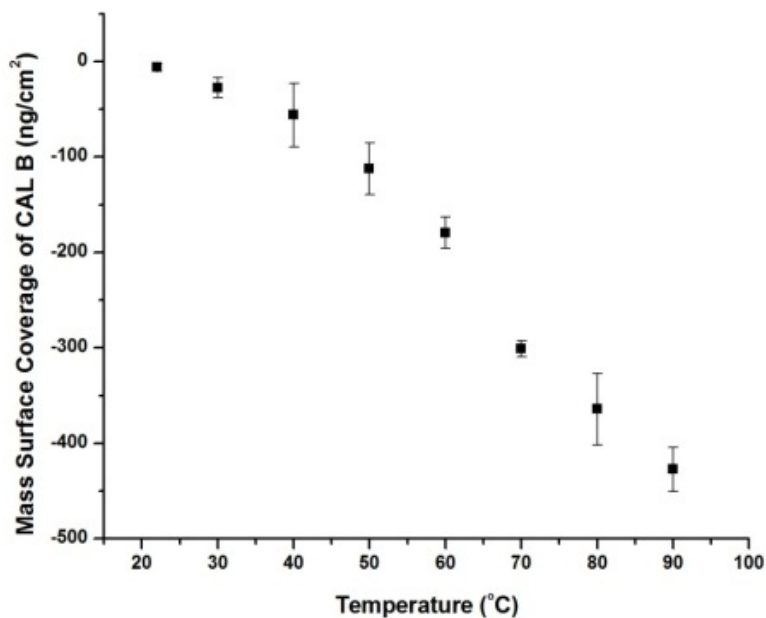


Figure 7. Net mass surface coverage of CAL B layer with increasing temperature of QCM-D module.

Effects of Buffer Ionic Strength on CAL B adsorption.

Various studies have looked at CAL B deposition onto polymer resins or surfaces using aqueous buffer solutions of varying ionic strength.^{18,19,21,45,46} Buffer ionic strength affects the solvation of the enzyme, which may impact enzyme adsorption on the solid support. A systematic study of enzyme adsorption onto the PMMA sensor surface with varying salt concentrations was conducted with several trials for each buffer system. The Sauerbrey mass was calculated for the third frequency overtone in each reaction and the average mass surface coverage of CAL B at buffer concentrations between 0.010 mol/L and 0.100 mol/L are displayed in Figure 8.

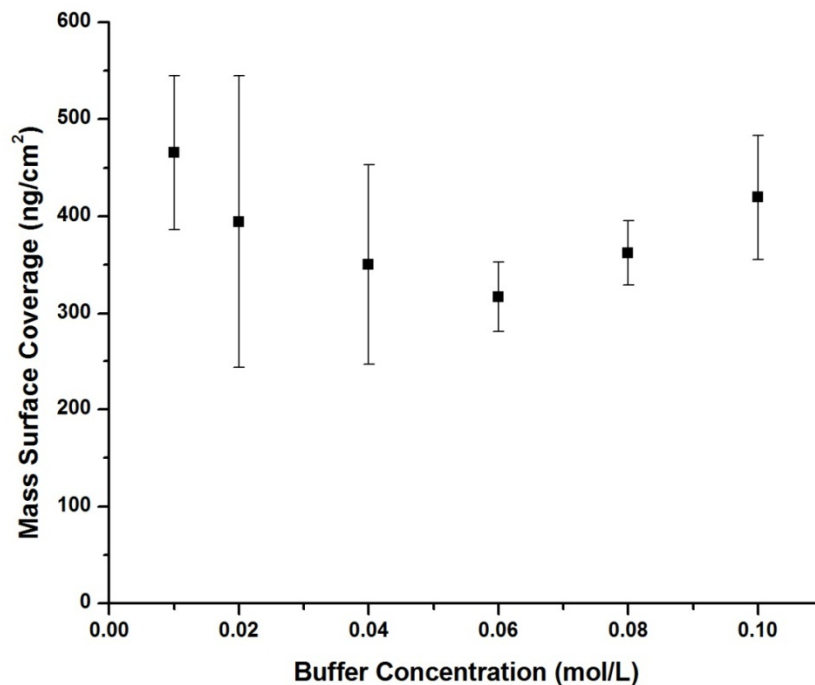


Figure 8. Net mass surface coverage of CAL B layer deposited in phosphate buffer (pH 7.0) with increasing salt concentration. The error bars represent one standard deviation of the data taken.

There is a decrease in enzyme adsorption for the intermediate salt concentrations (0.040 mol/L to 0.080 mol/L) and large standard deviation for adsorption at concentrations below 0.060 mol/L. This variation between low and high ionic strengths was further investigated by comparing frequency and dissipation data at 0.010 mol/L (Figure S4) and 0.100 mol/L (Figure S2) to determine if the CAL B layer is significantly different within the buffer environments. The dissipation change for all overtones is small for both 0.010 mol/L and 0.100 mol/L depositions at 1.0×10^{-6} . The frequency change for the 3rd, 5th, and 7th overtones in the 0.010 mol/L CAL B deposition spread significantly, indicating a more viscoelastic surface. A frequency versus

dissipation plot for CAL B adsorption in 0.010 mol/L and 0.100 mol/L give a qualitative evaluation of enzyme layer formation, shown in Figure S5, where the $\Delta f/\Delta D$ slope indicates a difference in the rigidity of the CAL B films. The 0.010 mol/L CAL B layer was modeled using standard Kelvin-Voigt viscoelastic models using the third, fifth, and seventh overtones in the model. The average Voigt mass calculated was greater than the Sauerbrey mass by 50 ng/cm², yielding a mass surface coverage of 517 ng/cm² \pm 44 ng/cm². The viscoelastic properties of the CAL B film determined a shear elastic modulus of 0.62 MPa \pm 0.2 MPa and a shear viscosity of 3.6 Pa s \pm 0.7 $\times 10^{-3}$ Pa s. The calculated loss modulus of the CAL B layer was 0.13 MPa, indicating the film is more elastic than viscous as $G' > G''$. The Kelvin-Voigt model of frequency and dissipation changes agreed well with experimental data, as χ^2 vector values were ≤ 20 and the modeled and experimental curves were nearly identical (Figure 9). These results indicate that the CAL B layer formed in low ionic strength buffer (0.010 mol/L) will be viscoelastic and less rigid than enzyme layers formed in high ionic strength buffer (0.100 mol/L). Further evaluation of enzyme activity in relation to enzyme rigidity must be conducted to determine if catalyst activity varies with the method of enzyme deposition on the polymer solid support.

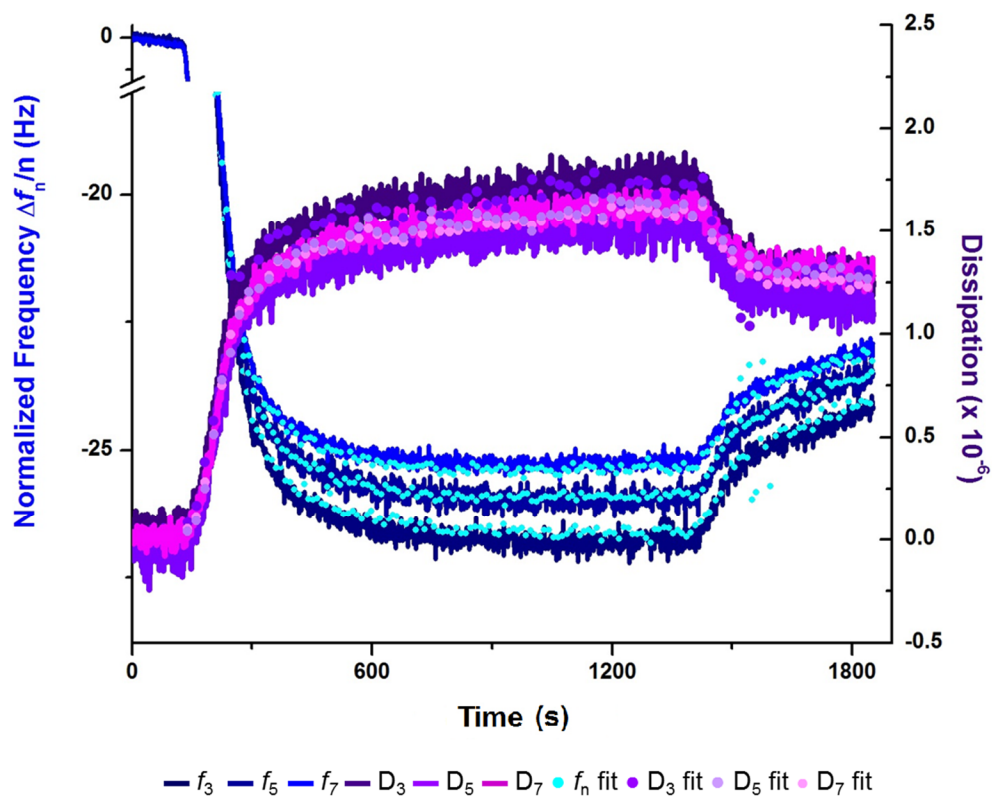


Figure 9. Adsorption of CAL B onto PMMA in 0.010 mol/L phosphate buffer, monitored by frequency (blue) and dissipation (purple) changes for 3rd, 5th, and 7th overtone. Voigt modeling of the fits for each overtone are represented by the dotted lines, where each dot is every 10th data point of the fitted curve.

Conclusions. A homogenous two-dimensional model of a crosslinked PMMA resin was fabricated on a quartz crystal microbalance sensor to monitor the adsorption and stability of CAL B catalyst interface in situ to changes in water concentration, addition of polymer, and changes in temperature. QCM-D of the PMMA/CAL B model probed the viscoelastic properties of the thin enzyme layer as it transitioned between viscoelastic and rigid conditions resulting from varied reaction environments. All QCM-D measurements are indicative of the chemical

affinity of CAL B for PMMA on a flat, smooth surface, which may be augmented by other forces and interactions induced by a porous particle geometry in the reaction environment of solid supported enzymes. Future studies of the CAL B/PMMA model may include activity studies through in situ titration with a catalyst inhibitor or the introduction of structure or patterning to the polymer surface.

The development of a homogenous crosslinked polymer surface through a dual photochemical approach can have a wide variety of applications for characterization of polymer interfaces. Fabrication of the model can be easily tuned with other commercially available polymers to characterize other biological adsorption and desorption processes at polymer surfaces.

ASSOCIATED CONTENT

AFM images, frequency, and dissipation QCM-D data are included in the Supporting Information. This material is available free of charge via the Internet at <http://pubs.acs.org>.

AUTHOR INFORMATION

Corresponding Author

*Kathryn L. Beers, Polymers Division, National Institute of Standards and Technology, Gaithersburg, Maryland 20899, United States. *Richard Gross, Polytechnic Institute of NYU, Brooklyn, New York 11201, United States

Present Addresses

† Dave C. Swalm School of Chemical Engineering, Mississippi State University, Mississippi State, Mississippi 39762

Author Contributions

The manuscript was written through contributions of all authors. All authors have given approval to the final version of the manuscript.

ACKNOWLEDGMENT

The authors gratefully acknowledge Christopher M. Stafford, Dongbo Wang, and Biolin Scientific for their assistance and advice on the PFQNM AFM and QCM-D. S. Orski wishes to acknowledge postdoctoral research support from the National Research Council Research Associateship Program.

REFERENCES

- (1) Tufvesson, P.; Lima-Ramos, J.; Nordblad, M.; Woodley, J. M. *Org. Process Res. Dev.* **2010**, *15*, 266–274.
- (2) Zhao, X. S.; Bao, X. Y.; Guo, W.; Lee, F. Y. *Mater. Today* **2006**, *9*, 32–39.
- (3) Kirschning, A.; Jas, G. In *Immobilized Catalysts*; Kirschning, A., Ed.; Topics in Current Chemistry; Springer Berlin / Heidelberg, 2004; Vol. 242, pp. 209–239.
- (4) Albertsson, A.-C.; Srivastava, R. K. *Adv. Drug Deliver. Rev.* **2008**, *60*, 1077–1093.
- (5) Kundu, S.; Bhangale, A. S.; Wallace, W. E.; Flynn, K. M.; Guttman, C. M.; Gross, R. A.; Beers, K. L. *J. Am. Chem. Soc.* **2011**, *133*, 6006–6011.
- (6) Gross, R. A.; Kumar, A.; Kalra, B. *Chem. Rev.* **2001**, *101*, 2097–2124.
- (7) Bhangale, A. S.; Beers, K. L.; Gross, R. A. *Macromolecules* **2012**, *45*, 7000–7008.
- (8) Johnson, P. M.; Kundu, S.; Beers, K. L. *Biomacromolecules* **2011**, *12*, 3337–3343.
- (9) Kundu, S.; Johnson, P. M.; Beers, K. L. *ACS Macro Lett.* **2012**, *1*, 347–351.
- (10) Mei, Y.; Kumar, A.; Gross, R. A. *Macromolecules* **2002**, *35*, 5444–5448.
- (11) Cheng, C. I.; Chang, Y.-P.; Chu, Y.-H. *Chem Soc Rev* **2012**, *41*, 1947–1971.
- (12) Ohlsson, G.; Tigerström, A.; Höök, F.; Kasemo, B. *Soft Matter* **2011**, *7*, 10749.
- (13) Höök, F.; Vörös, J.; Rodahl, M.; Kurrat, R.; Böni, P.; Ramsden, J.; Textor, M.; Spencer, N.; Tengvall, P.; Gold, J.; Kasemo, B. *Colloid. Surface. B* **2002**, *24*, 155–170.
- (14) Kao, P.; Allara, D. L.; Tadigadapa, S. *IEEE Sens. J.* **2011**, *11*, 2723–2731.
- (15) Liu, S. X.; Kim, J.-T. *J. Lab. Autom.* **2009**, *14*, 213–220.
- (16) Liu, C.; Meenan, B. J. *J. Bionic Eng.* **2008**, *5*, 204–214.
- (17) Reviakine, I.; Johannsmann, D.; Richter, R. P. *Anal. Chem.* **2011**, *83*, 8838–8848.
- (18) Laszlo, J. A.; Evans, K. O. *J. Mol. Catal. B-Enzym.* **2007**, *48*, 84–89.
- (19) Volden, S.; Moen, A. R.; Glomm, W. R.; Anthonsen, T.; Sjöblom, J. *J. Disper. Sci. Technol.* **2009**, *30*, 865–872.
- (20) Laszlo, J. A.; Evans, K. O. *J. Mol. Catal. B-Enzym.* **2009**, *58*, 169–174.
- (21) Loos, K.; Kennedy, S. B.; Eidelman, N.; Tai, Y.; Zharnikov, M.; Amis, E. J.; Ulman, A.; Gross, R. A. *Langmuir* **2005**, *21*, 5237–5241.

- (22) Prucker, O.; Naumann, C. A.; Rhe, J.; Knoll, W.; Frank, C. W. *J. Am. Chem. Soc.* **1999**, *121*, 8766–8770.
- (23) Cho, J.-H.; Lee, C.-W.; Gong, M.-S. *Polymer (Korea)* **1998**, *22*, 714.
- (24) Sauerbrey, G. *Z. Phys.* **1959**, *155*, 206–222.
- (25) Voinova, M. V.; Rodahl, M.; Jonson, M.; Kasemo, B. *Phys. Scripta* **1999**, *59*, 391–396.
- (26) Vogt, B. D.; Lin, E. K.; Wu, W.; White, C. C. *J. Phys. Chem. B* **2004**, *108*, 12685–12690.
- (27) Eisele, N. B.; Andersson, F. I.; Frey, S.; Richter, R. P. *Biomacromolecules* **2012**.
- (28) Rodahl, M.; Hok, F.; Fredriksson, C.; Keller, C. A.; Krozer, A.; Brzezinski, P.; Voinova, M.; Kasemo, B. *Faraday Discuss.* **1997**, *107*, 229–246.
- (29) Turro, N. J. *Modern Molecular Photochemistry*; University Science Books: Mill Valley, 1991.
- (30) Dhende, V. P.; Samanta, S.; Jones, D. M.; Hardin, I. R.; Locklin, J. *ACS Appl. Mater. Interfaces* **2011**, *3*, 2830–2837.
- (31) Pahnke, J.; Rhe, J. *Macromol. Rapid Commun.* **2004**, *25*, 1396–1401.
- (32) Shen, W. W.; Boxer, S. G.; Knoll, W.; Frank, C. W. *Biomacromolecules* **2000**, *2*, 70–79.
- (33) Naumann, C. A.; Prucker, O.; Lehmann, T.; Rhe, J.; Knoll, W.; Frank, C. W. *Biomacromolecules* **2001**, *3*, 27–35.
- (34) Toomey, R.; Freidank, D.; Rhe, J. *Macromolecules* **2004**, *37*, 882–887.
- (35) Leshem, B.; Sarfati, G.; Novoa, A.; Breslav, I.; Marks, R. S. *Luminescence* **2004**, *19*, 69–77.
- (36) Pakzad, A.; Simonsen, J.; Yassar, R. S. *Compos. Sci. Technol.* **2012**, *72*, 314–319.
- (37) Brandrup, J.; Immergut, E. H.; Grulke, E. A. *Polymer handbook*; Wiley: New York, 1999.
- (38) Marshall, G. P.; Coutts, L. H.; Williams, J. G. *J. Mater. Sci.* **1974**, *9*, 1409–1419.
- (39) Briscoe, B. J.; Sebastian, K. S. *Proc. R. Soc. Lond. A* **1996**, *452*, 439–457.
- (40) Vidyasagar, A.; Sung, C.; Gamble, R.; Lutkenhaus, J. L. *ACS Nano* **2012**, *6*, 6174–6184.
- (41) Bodvik, R.; Macakova, L.; Karlson, L.; Thormann, E.; Claesson, P. *Langmuir* **2012**, *28*, 9515–9525.
- (42) McLinden, M. O.; Splett, J. D. *J. Res. Natl. Inst. Stand. Technol.* **2008**, *113*, 29–67.
- (43) Santos, F. J. V.; Nieto de Castro, C. A.; Dymond, J. H.; Dalaouti, N. K.; Assael, M. J.; Nagashima, A. *J. Phys. Chem. Ref. Data* **2005**, *35*, 1–8.
- (44) Idris, A.; Bukhari, A. *Biotechnol. Adv.* **2012**, *30*, 550–563.
- (45) Chen, B.; Miller, E. M.; Miller, L.; Maikner, J. J.; Gross, R. A. *Langmuir* **2006**, *23*, 1381–1387.
- (46) Chen, B.; Pernodet, N.; Rafailovich, M. H.; Bakhtina, A.; Gross, R. A. *Langmuir* **2008**, *24*, 13457–13464.

Supporting Information for

Design and Implementation of Two-Dimensional Polymer Adsorption
Models: Evaluating the Stability of *Candida Antarctica Lipase B* at
Solid-Support Interfaces by QCM-D

Sara V. Orski,^a Santanu Kundu,^{a,†} Richard Gross,^{b,*} and Kathryn L. Beers^{a*}

^a Polymers Division, National Institute of Standards and Technology, Gaithersburg, Maryland
20899, United States

^b Polytechnic Institute of NYU, Brooklyn, New York 11201, United States

† Dave C. Swalm School of Chemical Engineering, Mississippi State University, Mississippi
State, Mississippi 39762

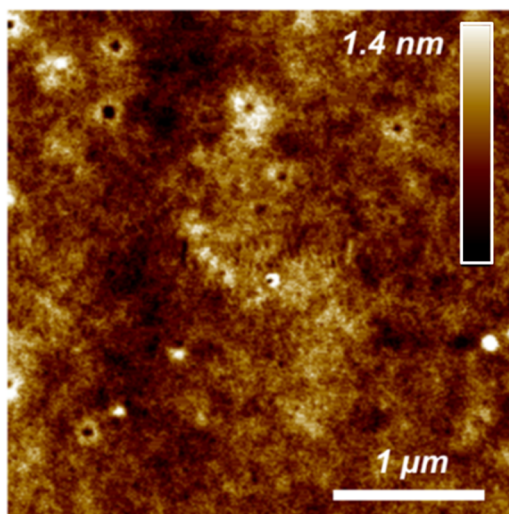


Figure S1. Representative height image of crosslinked PMMA film (50 nm) on a quartz crystal sensor surface. The color scale represents the height of the film from 0 nm to 1.4 nm.

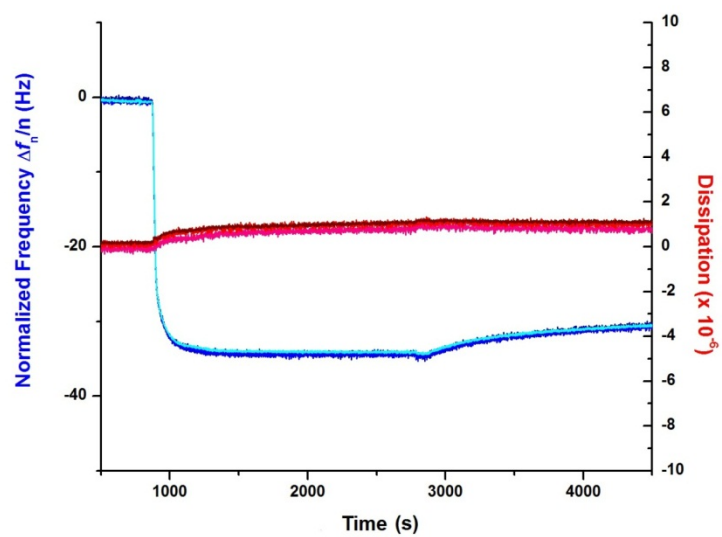


Figure S2. QCM frequency and dissipation changes upon CAL B adsorption on PMMA in 0.100 mol/L buffer.

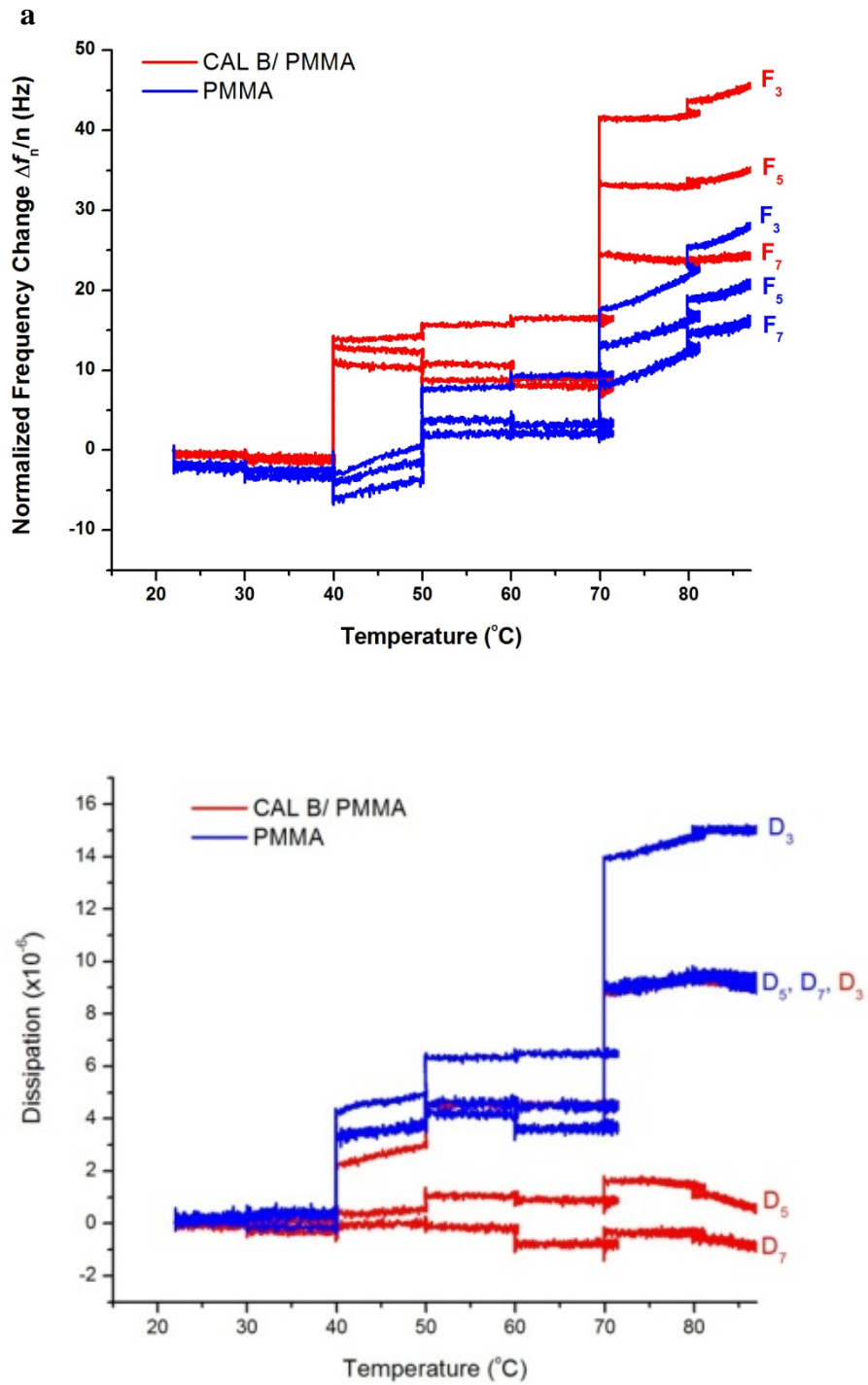


Figure S3. Temperature-dependent frequency (a) and dissipation (b) changes to CAL B and unmodified PMMA sensors corrected for effects of the bare crystal.

Table S1. Ratio of dissipation to frequency at the third overtone ($n=3$) for final response of corrected CAL B at temperature. A ratio of less than 4×10^{-7} is indicative of a rigid layer.

Temperature, °C	$\Delta D_n/(-\Delta f_n/n)$, ($\times 10^7$)
22	0.00
30	2.86
40	3.53
50	4.40
60	5.00
70	5.31
80	6.54
90	5.85

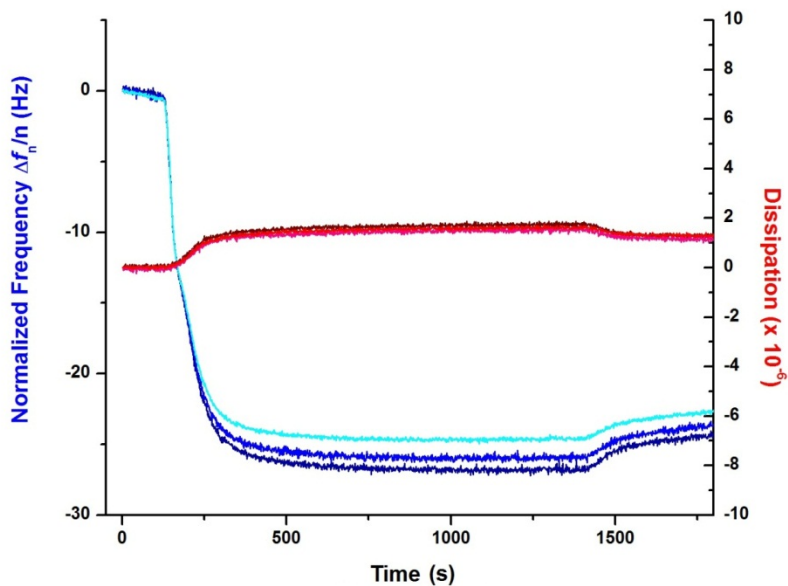


Figure S4. QCM frequency and dissipation changes upon CAL B adsorption on PMMA in 0.010 mol/L buffer.

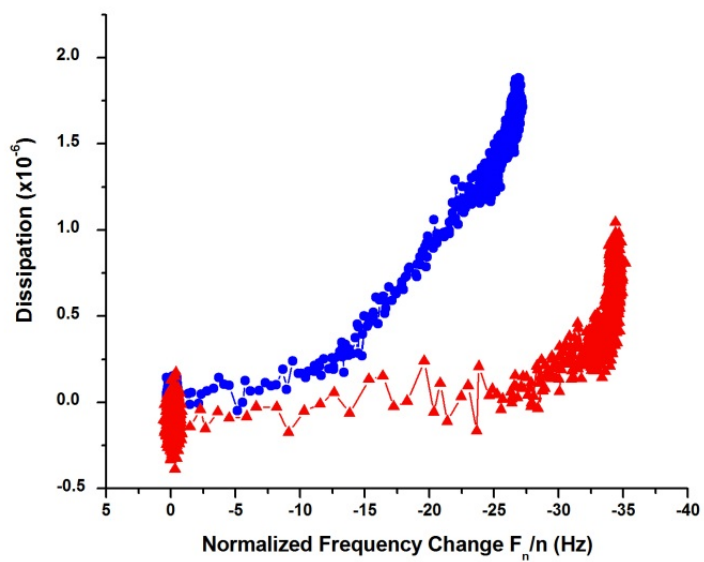


Figure S5. Frequency versus dissipation plots for CAL B adsorption in 0.01 mol/L (●) and 0.100 mol/L (▲) buffer.

Table of Contents Graphic:

